

# Conceptualising the behaviour of 3D printed concrete structures in fire

Selicia Pillay (1), Richard S. Walls (1) and Johann E. van der Merwe (2)

(1) Department of Civil Engineering, Stellenbosch University

(2) Department of Civil Engineering, University of Pretoria

## Abstract

Three-dimensional printed concrete (3DPC) is becoming a growing alternative to traditional construction practices. In recent years this novel technique has been developed into practical construction applications, including structures such as façade panels, bridges, houses, and office buildings. Despite the considerable endeavours of academia and industry towards the advancement of 3DPC practices, existing knowledge on the structural behaviour of 3DPC in fire is limited. The structural performance of non-loadbearing 3DPC cavity walls were reported in this paper using appropriate numerical uncoupled thermo-mechanical models. The aim of this work is to conceptualise both thermal performance and thermally induced stresses in 3DPC walls exposed to elevated temperatures. Using free-body diagrams of typical 3DPC walls to evaluate numerical results, it is shown that significant internal stresses can develop, which are likely to cause extensive cracking with vertical cracking (perpendicular to printed concrete layers) being dominant rather than horizontal cracking, as may be expected.

**Keywords:** 3D-printed concrete; finite element modelling; fire performance; structural damage; standard fire.

## 1. INTRODUCTION

In comparison to other global industries, the construction sector has been slower to adopt new technologies [1]. Faced with skill scarcity, an expanding number of projects, and the need to limit its environmental impact, the construction industry is progressing to automation to improve productivity, cost efficiency, and reduce material waste. Automation revolutions, such as 3D printing, can transform the construction industry. Due to the novelty of 3DPC, limited research has been compiled regarding the structural behaviour of 3DPC in a fire. Therefore, this paper intends to develop an understanding of the behaviour in common wall configurations of 3DPC in a fire. The study serves as an important first step in guiding future research and identifying potential modes of failure that must be investigated through full-scale furnace testing and will potentially need design solutions developed for them.

## **2. THERMAL AND MECHANICAL PROPERTIES OF 3DPC**

Thermal finite element analysis of 3DPC elements is reliant on the key influencing characteristics of the material's temperature-dependent thermal properties [2]. The thermal conductivity, specific heat, and relative density variations with elevated temperature govern the thermal behaviour of a material. The Eurocode for the design of concrete in fire, EN 1992-1-2 [3], provides the thermal properties at elevated temperatures for traditional concrete materials. Suntharalingam et al [4] showed an almost equivalent relationship between the proposed thermal properties of 3DPC and EN-1992-1-2 properties at elevated temperatures, which was used in this study to develop the finite element model. It is beneficial that preliminary research indicates that new thermal models for 3DPC materials do not need to be developed, although details regarding mechanical resistance require further research.

The mechanical properties of 3DPC samples (compressive, and flexural tensile strength) are significantly influenced by the bonding behaviour at the interlayers of the 3DPC [5]. A comparative study of various authors [6-10] was conducted in to consider a range of mechanical properties to consider for this study. The peak compressive stress assumed in this study is 40 MPa with a maximum flexural strength of 4 MPa. The density of the 3DPC at ambient temperature is assumed to be 2300 kg/m<sup>3</sup>. The study considered isotropic material to allow a preliminary investigation of the behaviour. However, 3DPC anisotropic should be included in future work, as it will influence the maximum stresses than can be achieved in each direction, especially between layers. Despite this limitation, the study clearly highlights the susceptibility of fire-induced damage to inner layers of 3DPC wall panels.

## **3. DEVELOPMENT OF THE FINITE ELEMENT MODEL**

In this work, a 3D finite element numerical model was developed in Abaqus [11] to evaluate the structural response of 3DPC wall panels with various cross-sectional patterns. The study considered non-load bearing 3DPC wall configurations and performed a decoupled heat transfer and mechanical analysis. The numerically investigated thermo-mechanical behaviour of the advanced wall configurations was based on the currently available geometries of 3DPC walls in the construction industry and the cavity provisions proposed by Wang et al (2012) [12] (Figure 1). All wall configurations are 1 000 mm high and 200 mm thick with the exposed and unexposed panels (external strip width) kept the same width (35 mm).

A heat transfer time step with a time of 3600 seconds (60 minutes) was created for the evaluation period, with an ISO 834 standard time-temperature used to define the exposed face gas temperature. This duration was considered adequate to illustrate the objectives of this work and is sufficient for the majority of buildings (such as offices, residential and institutional buildings), except high-rise buildings. Figure 2 shows the detailed input of the heat transfer mechanisms that take place within a typical cross-section configuration. The external and internal predefined temperature was set at 20°C (ambient temperature). The time-temperature profile measured from the heat transfer analysis of all the cross-sections are applied as predefined fields to the perspective cross-sections over a normalized time

period in the mechanical analysis. Parameters for convection, cavity radiation and the general configuration for heat flow are also indicated on Figure 2.

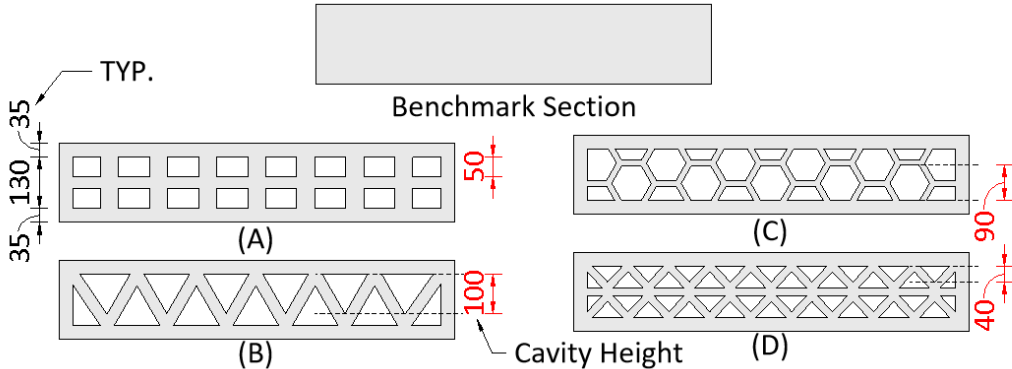


Figure 1: Wall configurations used in this study: (Top) Benchmark Section, (A) Cross-section A - lattice, (B) Cross-section B - truss, (C) Cross-section C - cellular, and (D) Cross-section D - triangular (unit: mm). Dimensions shown in red indicate cavity depths.

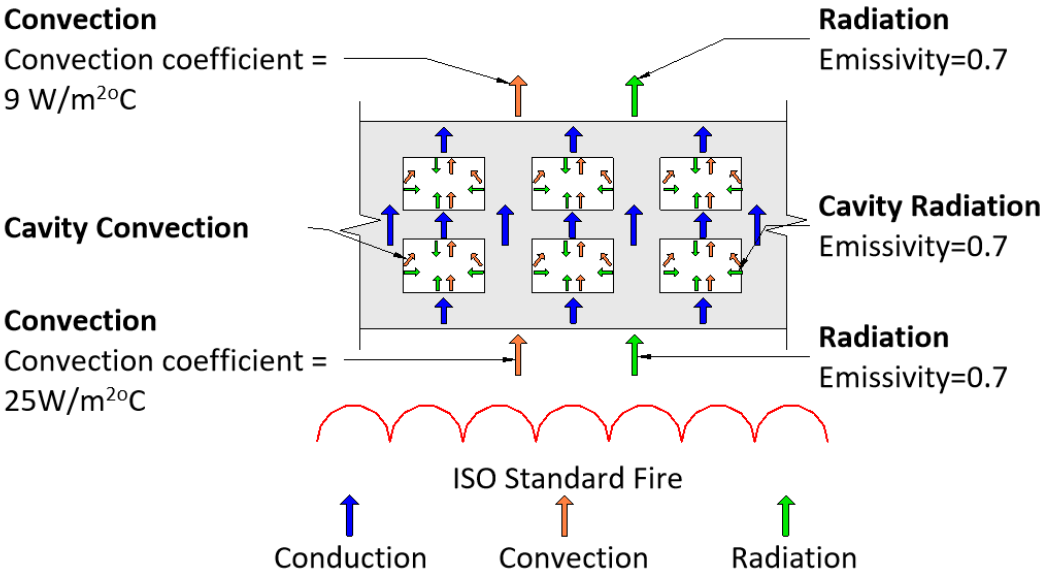


Figure 2: Heat transfer assumptions for the Abaqus [11] models.

**4. THERMAL BEHAVIOUR OF 3DPC CAVITIES**

**4.1. Consideration of Fire Resistance**

The fire performance of a structure or element is its ability to perform its design purpose in the event of a fire over a specific duration. The requirements for fire resistance are stability, integrity, and insulation. The insulation behaviour for similar wall configurations has been thoroughly investigated by Suntharalingam et al [4], who used the unexposed panel

temperature to investigate the insulation behaviour according to EN 1992-1-2 [3]. To satisfy the insulation criterion the unexposed panel should not exceed an average of 140°C and 200°C at any point on the unexposed surface.

#### 4.2. Wall Panel Temperatures

Figure 3 depicts a comparison of the exposed surface temperatures of each cross-section with respect to time after 60 minutes of fire exposure. A higher front surface face temperature indicates a sample with a lower rate of heat transfer through it, i.e., it is a better insulator. This may be either positive or negative. Samples with lower temperature gradients (i.e., that let the heat through more rapidly) will fail fire test insulation requirements more quickly (140°C above ambient). However, higher temperature gradients lead to higher levels of induced thermal stresses, as the degree of thermal expansion between the front and back face differ more greatly.

As expected, a maximum temperature of 919°C is observed in Cross-section C (cellular) (i.e., close to the standard fire curve temperature of 945°C). This cellular configuration results in lowest resultant effective conductivity, with the mechanics discussed further below. The minimum exposed face temperature was observed in the cast solid section with a temperature of 895°C at 60 minutes. Figure 4 depicts the unexposed surface panel of the various wall cross-sections. It appears that the temperature curves follow an approximately exponential trend for all cross-sections. Cross-section B (truss) produced the maximum temperature on the unexposed surface of 43°C. All cross-sectional overall widths were kept the same to ensure consistency and not be a governing factor in the fire performance of the wall.

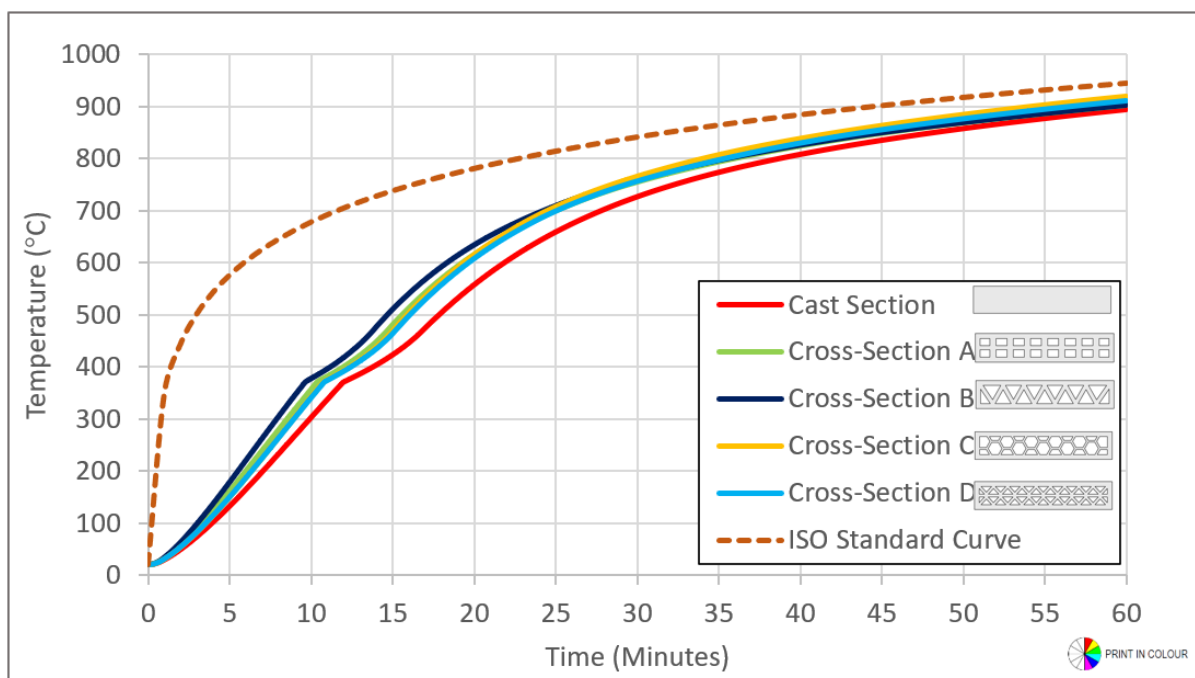


Figure 3: Exposed surface temperature for each wall configuration. No substantial differences noted between various cross-section geometry.

Heat transfer is based on the rate at which energy can flow through the system. Since energy can either be transferred by conduction (in solid sections) or convection and radiation (in cavities) the relative rate of heat transfer will vary. Cavity radiation is instantaneous in that as soon as the fire-exposed side of a cavity heats up it leads to energy transfer to the far side. However, the rate of transfer may be lower than conduction, depending on the distance covered. For deep cavities, cavity radiation results in more rapid transfer. When there are multiple layers of material the heat transfer mechanism sequence can be (1) conduction, (2) cavity radiation, (3) conduction, (4) cavity radiation, and (5) conduction. However, each intermediate layer will radiate back and transfer heat back to the fire-exposed side, leading to reduced energy transfer through the section. Hence, there is a complex, non-linear interaction of these factors depending on the geometry and heat transfer mechanisms, leading to some cross-sectional shapes heating faster than others.

Cross-section B (truss) showed the lowest performance in terms of insulation due to producing the highest temperature on the unexposed surface. This occurs as there is effectively one line of cavities to cross (albeit the cavities change in width). Cross-section C (Cellular) and Cross-section D (double layer triangular) displayed increased insulation performance due to producing a relatively low temperature on the unexposed surface. It is observed that Cross-section A (double layer lattice), Cross-section C (cellular) and Cross-section D (double layer triangular) had lower unexposed surface temperatures than the solid section, and this can be attributed to the air within the cavity reducing the heat transmission along with the thermal radiant feedback from multiple concrete lamina.

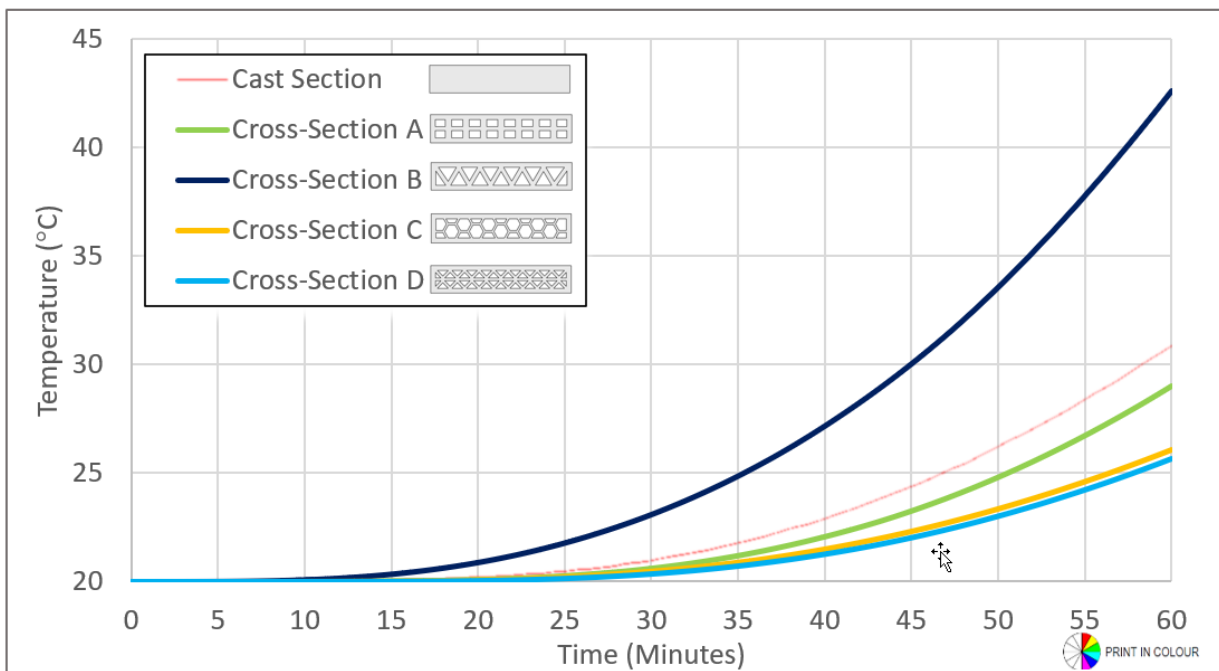


Figure 4: Unexposed surface temperature for each wall configuration.

All the cross-sections investigated pass the fire resistance insulation criterion of the unexposed face, with the highest temperature ( $43^{\circ}\text{C} = 23^{\circ}\text{C}$  above ambient) still being significantly below the requirement of around  $140^{\circ}\text{C}$  above ambient. Hence, from a thermal perspective a two-hour fire rating could potentially be attained by these samples. However, of great concern is the very high thermal gradients encountered, with changes in temperature of almost  $900^{\circ}\text{C}$  across sections which will lead to extensive internal stresses, as will now be discussed.

**4.3. Stress-Strain Relationship of 3DPC Cavities**

Due to the complex nature of the wall’s configuration geometry, the behaviour of the stresses in 3DPC has not been extensively researched. As a first step this work proposes a simple free-body diagram, based on fundamental mechanics, for outlining the magnitude of stresses that might be expected during fire. Figure 5 illustrates the fundamental structural mechanics that occurs in a typical cavity cross-section which drives cracking.

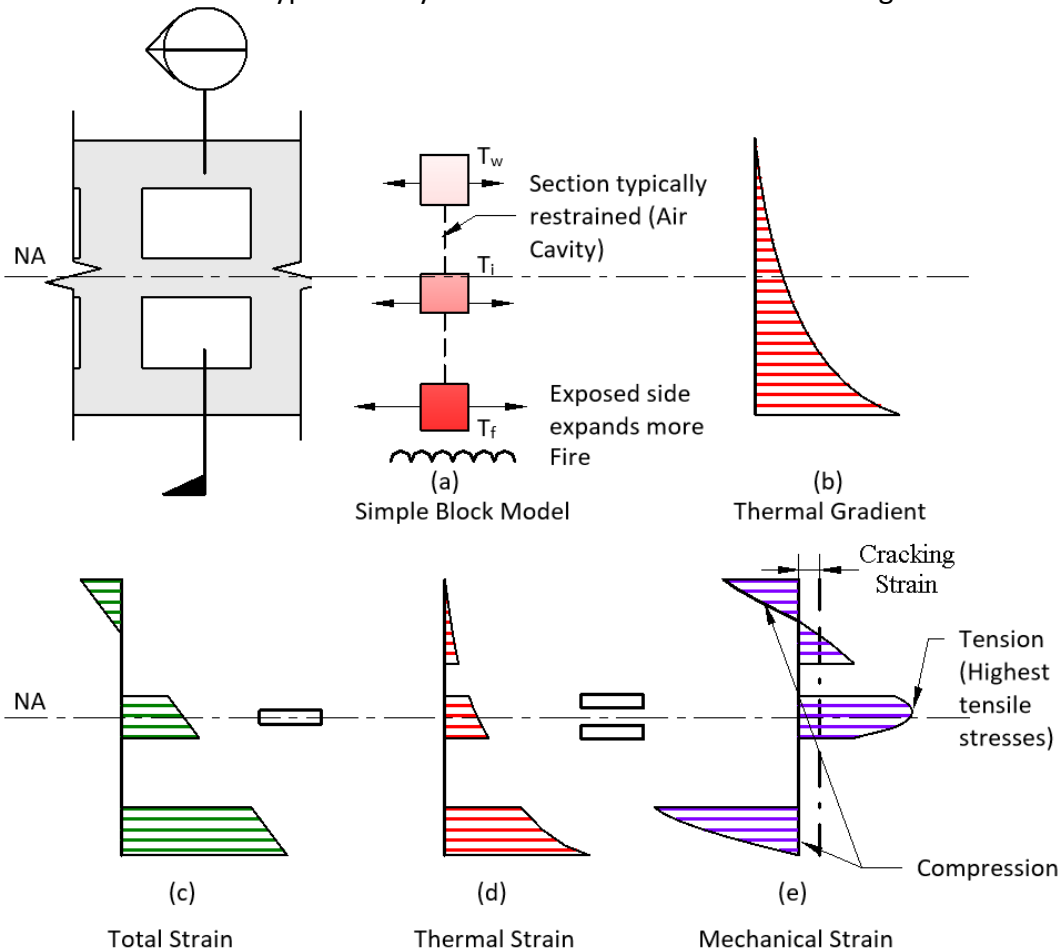


Figure 5: Type C Cross-section, showing (a) the simple block model, (b) the temperature profile, (c) the total strain is (d) subtracted from thermal strain and (e) indicates the complex mechanical strain profile.

The upper portion of the diagram indicates the cross-section (left), temperature profile (b) (right) and how the cross-section has been simplified into three layers (a). Assuming simple Euler-Bernoulli behaviour holds, the total strain in a cross-section will be as shown in (c). Considering that thermal strain is approximately proportional to the temperature, the thermal strain profile is as given in (d). The mechanical strain is the difference between the total and thermal strains. Depending on the temperature, and material model adopted, the mechanical stress (i.e., stress that results in structural elongations and cracking) will be approximately as shown in diagram (e).

From this diagram we see the first onset of cracking occurring in the internal middle layer, as depicted in Figure 5(e). Based on finite element models the time to onset of cracking ranged from 3 minutes for Cross-section A and D to 15 minutes for Cross-section B. This was influenced by the geometric distance from the exposed panel, resulting in the different onset of cracking times. It is of significant concern that simple models, and a free-body diagram based on fundamental structural mechanics, indicate that vertical cracking is likely to occur very quickly in sections. Also, it appears that cracking will start within the sample, rather than at the sample face, due to the thermal gradients and section geometries.

## 5. CONCLUSION

The work presented in this paper highlights a fundamental issue with the use of 3DPC and the thermal behaviour associated with it. The structural mechanics occurring within the 3DPC cavity walls are presented to illustrate the complex stress-strain relationship at elevated temperatures. The simplified illustrations of the internal stress and strain profiles are important for understanding why internal cracking may occur, and the predicted stress profiles, can be applied to various cross-sections in future work to identify the onset cracking. This is fundamentally important for post-fire damage assessment and consideration in the design process of the structure. Further investigations and research should be conducted into the thermal and associated mechanical behaviour of 3DPC walls. With 3DPC walls typically having low tensile strength (i.e. no reinforcement) this aspect should be investigated to consider whether 3DPC structures are as robust in fire as might be expected.

## 6. REFERENCES

- [1] World Economic Forum, "Shaping the Future of Construction: A Breakthrough in Mindset and Technology," World Economic Forum, Geneva, 2016.
- [2] Y. Weng, M. Li, Z. Liu, W. Lao, B. Lu, D. Zhang and M. Tan , "Printability and fire performance of a developed 3D printable fibre reinforced cementitious composites under elevated temperatures," *Virtual and Physical Prototyping*, vol. 14, no. 3, pp. 284-292, 2019.
- [3] CEN, Design of concrete structures-Part 1-2: General rules-Structural fire design, 1 ed., Brussels: European Committee for Standardization, 2004.

- [4] T. Suntharalingam, P. Gatheeshgar, I. Upasiri, K. Poologanathan and B. Nag, "Fire performance of innovative 3D printed concrete composite wall panels – A Numerical Study," *Case Studies in Construction Materials*, vol. 25, no. 2, pp. 705-716, 2021.
- [5] T. Bui, "Buildability and Mechanical Properties of 3D Printed Concrete," *Materials*, vol. 13, no. 21, pp. 1-24, 2020.
- [6] D. Heras, M. Moneeb and M. R. Taha, "Examining the significance of infill printing pattern on the anisotropy of 3D printed concrete," *Construction and Building Materials*, vol. 262, no. 1, p. 120559, 2020.
- [7] T. T. Le, S. Austin, S. Lim, R. Buswell, R. Law, A. Gibb and T. Thorpe, "Hardened properties of high-performance printing concrete," *Cement and Concrete Research*, vol. 42, no. 3, pp. 558 - 566, 2012.
- [8] V. N. Nerella, M. Krause, M. Näther and V. Mechtcherine, "Studying printability of fresh concrete for formwork free Concrete on-site 3D Printing technology (CONPrint3D)," Regensburg, 2016.
- [9] B. Panda, S. C. Paul, N. A. Noor and Y. D. Tay, "Measurement of tensile bond strength of 3D printed geopolymer mortar," *Measurement*, vol. 113, no. 2018, pp. 108-116, 2018.
- [10] Y. Zhang, Y. Zhang, L. Yang, G. Liu, Y. Chen, S. Yu and H. Du, "Hardened properties and durability of large-scale 3D printed cement-based materials," *Materials and Structures*, vol. 54, no. 45, pp. 1-114, 2021.
- [11] Dassault Systèmes, *Abaqus Unified FEA (Abaqus 2021)*, Providence, RI: Dassault Systèmes, 2021.
- [12] Y. Wang, I. Burgess, F. Wald and M. Gillie, *Performance-based fire engineering of structures*, 1st ed., New York: Spon Press, 2012.